

1 **Coupling state-of-the-art modelling tools for better informed Red List assessments of**
2 **marine fishes**

3
4 **Arnaud Grüss^{a, b*}, Henning Winker^c, James T. Thorson^d, Nicola D. Walker^e, Aurore**
5 **Maureaud^f, Nathan Pacoureaux^g**

6
7 ^a University of Washington School of Aquatic and Fishery Sciences, Seattle, WA, USA.

8
9 ^b NIWA, Wellington, New Zealand.

10
11 ^c Department of Aquatic Resources, Institute of Marine Research, Swedish University of
12 Agricultural Sciences, Sweden

13
14 ^d Habitat and Ecological Processes Research program, Alaska Fisheries Science Center,
15 NOAA Fisheries, Seattle, WA, USA.

16
17 ^e Cefas, Lowestoft Laboratory, Pakefield Road, Lowestoft, UK

18
19 ^f Rutgers University Department of Ecology Evolution and Natural Resources, New
20 Brunswick, NJ, USA

21
22 ^g Earth to Ocean Research Group, Biological Sciences, Simon Fraser University, Burnaby,
23 BC, Canada

24
25 ****Correspondence author***

26 Arnaud Grüss

27 NIWA

28 301 Evans Bay Parade

29 Greta Point, Wellington 6021, New Zealand

30 Email: Arnaud.Gruss@niwa.co.nz

31 **Acknowledgments**

32 We thank very much Romain Frelat for assisting us in preparing survey data. We are
33 very grateful to José de Oliveira and Jim Ellis for their expert review and to Olaf Jensen, the
34 Editor (Tadeu Siqueira), the Associate Editor (Caren Barceló) and three anonymous reviewers
35 for their comments, which all considerably improved the quality of the manuscript. We also
36 thank very much Lydia Groves for all of her assistance during the reviewing and production
37 processes. Reference to trade names does not imply endorsement by the National Marine
38 Fisheries Service, NOAA. The scientific results and conclusions, as well as any views or

39 opinions expressed herein, are those of the author(s) and do not necessarily reflect those of
40 NOAA or the Department of Commerce.

41

42 **Conflict of interest statement**

43 None of the authors have a conflict of interest.

44 **Authors' Contributions**

45 Arnaud Grüss, Henning Winker and James T. Thorson conceived the study; Arnaud Grüss,
46 Henning Winker, James T. Thorson and Nathan Pacoureau developed the models; Arnaud
47 Grüss and Aurore Maureaud compiled the data; Arnaud Grüss, Nicola D. Walker and Nathan
48 Pacoureau compared the results for the application to results from previous assessments and
49 studies; Arnaud Grüss, Henning Winker, James T. Thorson, Nicola D. Walker, Aurore
50 Maureaud and Nathan Pacoureau analysed and discussed the results and contributed to the
51 manuscript.

52

53 **Data availability statement**

54 Data are available from the Figshare Digital Repository
55 <https://doi.org/10.6084/m9.figshare.22596799.v1> (Grüss, 2023). R codes are available from
56 the Zenodo Digital Repository <https://doi.org/10.5281/zenodo.10565146> (Grüss, 2024).

57 **Abstract**

58 **1.** In the face of biodiversity loss worldwide, it is paramount to quantify species' extinction
59 risk to guide conservation efforts. The International Union for the Conservation of Nature
60 (IUCN)'s Red List is considered the global standard for evaluating extinction risks. IUCN
61 criteria also inform national extinction risk assessments. Bayesian models, including the state-
62 of-the-art JARA ("Just Another Red List Assessment") tool, deliver probabilistic statements
63 about species falling into extinction risk categories, thereby enabling characterisation and
64 communication of uncertainty in extinction risk assessments.

65 **2.** We coupled the state-of-the-art VAST ("Vector Autoregressive Spatio-Temporal")
66 modelling tool and JARA, for better informed Red List assessments of marine fishes. In this
67 framework, VAST is fitted to scientific survey catch rate data to provide indices to JARA
68 whose uncertainty is propagated to JARA outcomes suggesting extinction risk categories
69 (under the population reduction criterion). In addition, VAST delivers a valuable habitat
70 assessment to better understand what may be driving extinction risk in the study region. Here,
71 we demonstrate the coupled VAST-JARA modelling framework by applying it to five
72 contrasting North Sea species, with or without a quantitative stock assessment and with
73 different conservation statuses according to the latest global Red List assessments.

74 **3.** The North Sea application coupled with previous assessments and studies suggest that,
75 among the three elasmobranchs, starry ray is in most need for urgent research (and
76 conservation actions where appropriate), followed by spurdog, whilst lesser-spotted dogfish is
77 increasing in biomass. Moreover, both the VAST-JARA modelling framework and previous
78 research indicate that, while European plaice is not of conservation concern, cod has likely
79 met the IUCN criteria for being listed as Endangered recently.

80 **4. *Synthesis and applications.*** The predictions of the VAST-JARA modelling framework for
81 North Sea species, including JARA output and VAST habitat assessment, constitute valuable

82 supporting information to make interpretations based on Red List guidelines, which will help
83 decision-makers in their next North Sea Red List assessment. We foresee applications of the
84 modelling framework to assist Red List assessments of numerous marine fishes worldwide.
85 Our modelling framework has many potential advantageous uses, including informing
86 resource management about climate change impacts on species' extinction risks.

87

88 **Keywords:** Red List assessments, state-space models, VAST, JARA, habitat assessment,
89 survey data, fishes

90 **Introduction**

91 In the face of biodiversity loss worldwide, it is paramount to quantify species’
92 extinction risk to guide conservation efforts (Hoffmann et al., 2008; Butchart et al., 2010).
93 The International Union for the Conservation of Nature (IUCN)’s Red List of Threatened
94 Species (“Red List”) is considered the global standard for evaluating species’ extinction risks
95 (Mace et al., 2008; Regan et al., 2013). IUCN criteria also inform national assessments of
96 species’ conservation status and extinction risk, such as the Committee on the Status of
97 Endangered Wildlife in Canada (COSEWIC)’s assessment of endangerment under the Species
98 at Risk Act (COSEWIC, 2019). Red List assessments are currently widely used to assess
99 progress towards United Nations Sustainable Development Goals and to set Biodiversity
100 Targets of the Convention on Biological Diversity. Following IUCN criteria, Red List
101 assessments classify species into extinction risk categories: Critically Endangered (CR),
102 Endangered (EN), Vulnerable (VU) (threatened categories), Near Threatened (NT), or Least
103 Concern (LC). It is important to note that numerous species are also classified as Data
104 Deficient (DD), i.e., that the extinction risk of numerous species cannot be assessed due to a
105 lack of data yet many of those non-assessed species may be threatened (IUCN, 2023).

106 Although there exist five IUCN criteria (A to E; IUCN, 2023), Criterion A (the rate of
107 population reduction scaled by generation length) is the most frequently and, often, the only
108 criterion employed for the Red List assessments of marine fishes (d’Eon-Eggertson et al.,
109 2015; Rueda-Cediel et al., 2018). This is primarily because Criterion A generally matches the
110 population statuses predicted by stock assessments (Davies & Baum, 2012; Pacoureau et al.,
111 2021). Different tools are available for assisting the Red List assessments that are based on
112 Criterion A, including very rapid and easy-to-use approaches. However, misclassifying
113 populations on the Red List can have substantial impacts on the prioritisation of conservation
114 efforts and, consequently, on our ability to optimally counter biodiversity loss (Ale & Mishra,

115 2018; Rueda-Cediel et al., 2018). Therefore, analysts should seek to carry out the Red List
116 assessments that are based on Criterion A (henceforth simply “Red List assessments”) with
117 tools that adequately characterise and communicate uncertainty around extinction risk.

118 Bayesian models represent powerful tools to evaluate extinction risks as they deliver
119 probabilistic statements about species falling into extinction risk categories, thereby
120 improving the characterisation and communication of uncertainty in extinction risk
121 assessments (Boyd et al., 2017; Post et al., 2022). Currently, Red List assessments for marine
122 fishes are generally supported by Bayesian state-space models implemented with the JARA
123 (“Just Another Red List Assessment”) platform, because of JARA’s capacity to incorporate
124 process error and uncertainty into the assessments (Sherley et al., 2020; Winker et al., 2020).
125 One major advantage of JARA is that it is less sensitive to outliers (due to process and
126 observation error) than simpler regression approaches and, therefore, more accurately
127 captures rates of population change (Sherley et al., 2020; Winker et al., 2020). One of JARA’s
128 main utilities is an easy-to-interpret graphic showing the probability of population decline
129 against Red List categories. This graphic, along with other JARA products, provides
130 practitioners with valuable insights into the weight of evidence that supports their Red List
131 assessment (Winker et al., 2020). JARA has been employed to assist Red List assessments for
132 around 100 elasmobranchs worldwide and other taxa including demersal bony fishes (da Silva
133 et al., 2019; Sherley et al., 2020; Dulvy et al., 2021; Pacoureau et al., 2021, 2023).

134 JARA inputs include abundance data and an estimate of generation length (the average
135 age of breeding individuals). For marine fishes, abundance data can come in the form of the
136 abundance trajectories predicted by stock assessment models or indices of relative abundance
137 (henceforth simply “indices”) derived from scientific survey catch rates or fisheries catch
138 rates (Winker et al., 2020), where abundance is either abundance in numbers or abundance in
139 biomass (henceforth simply “biomass”). Because most fish species worldwide do not have a

140 stock assessment (Ovando et al., 2021; RAM Legacy Stock Assessment Database, 2021),
141 indices are the most utilised data for JARA for marine fishes. Moreover, when available,
142 indices estimated from survey catch rates are preferred to indices estimated from fisheries
143 catch rates, because the stratified sampling design and well-defined sampling protocol (in
144 terms of methods and effort) of most surveys result in catch rates that are more representative
145 of the fish populations (National Research Council, 1998; Dennis et al., 2015). Indices are
146 generated from catch rates via a catch rate standardisation procedure using regression models
147 (Maunder & Punt, 2004).

148 Whilst numerous different models are available for catch rate standardisation (Hoyle et
149 al., 2024), there is increasing recognition of the critical role of spatial structure in species'
150 dynamics, extinction risks and recovery potential (Wilson et al., 2023). In this context, spatio-
151 temporal models, regression models that account for spatial and spatio-temporal structure, are
152 increasingly preferred for catch rate standardisation (Thorson et al., 2020). Spatio-temporal
153 models represent spatial variation (latent variation that is constant over time) and spatio-
154 temporal variation (latent variation that varies among years) at a very fine scale and,
155 therefore, result in very precise estimates via the borrowing of information across adjacent
156 locations and years (Shelton et al., 2014; Thorson et al., 2015). Simulation experiments also
157 indicate that, compared to simpler regression models, spatio-temporal models generally
158 produce more accurate estimates and/or better characterise uncertainty around these estimates
159 (Grüss et al., 2019b; Brodie et al., 2020). One major advantage of spatio-temporal models is
160 that, in addition to generating indices, they shed light on the spatio-temporal density patterns
161 and patterns of distribution shifts and range expansion/contraction of fishes (Thorson et al.,
162 2016). Thus, spatio-temporal models can deliver a habitat assessment (e.g., information about
163 changes in species' range) that complements JARA outputs for better informed Red List
164 assessments, as JARA informs only about species' extinction risks in relation to population

165 trends. One of the most widely used spatio-temporal modelling approaches is the VAST
166 (“Vector Autoregressive Spatio-Temporal”) state-space modelling tool (Thorson, 2019),
167 which is now commonly employed worldwide for the standardisation of the survey catch rates
168 of fishes (e.g., Hodgdon et al., 2020; O’Leary et al., 2020; Adams et al., 2021).

169 Here, we couple the state-of-the-art VAST and JARA state-space modelling tools for
170 better informed Red List assessments of marine fishes. VAST is fitted to survey catch rate
171 data to provide indices to JARA, but also density maps and other habitat information to better
172 understand what may be driving extinction risks in the study region. We demonstrate our
173 coupled VAST-JARA modelling framework by applying it to five contrasting North Sea
174 species.

175

176 **Materials and methods**

177 VAST

178 The VAST generalised linear mixed modelling platform was originally developed to
179 standardise fish catch rate data, which generally include many zeros (Thorson et al., 2015). As
180 such, VAST was designed as a delta modelling platform, that is a framework that combines
181 together the encounter probabilities estimated by a first linear predictor and the positive catch
182 rates estimated by a second linear predictor (Lo et al., 1992).

183 VAST delta models fitted to survey catch rate data estimate two linear predictors at
184 each site and in each year in the logarithm scale, as a function of: (1) year intercepts treated as
185 fixed effects; (2) spatial variation terms treated as random effects; (3) spatio-temporal
186 variation terms treated as random effects; and, potentially (4) density covariates and/or
187 catchability covariates (covariates related to sampling). The product of the two linear
188 predictors is equal to density, d . The spatial and spatio-temporal variation terms represent the
189 core of VAST models and account, respectively, for latent static and latent dynamic variables

190 that influence fish densities (Shelton et al., 2014; Thorson et al., 2015). Details about the
191 estimation and evaluation procedures of VAST models can be found in Appendix S1 in
192 Supporting Information.

193 The densities predicted by VAST models at each site s and in each year t , $d(s, t)$, can
194 be summed up over space to produce indices, $I(t)$, which can then be provided as input to
195 JARA. However, VAST model predictions can also be processed to deliver a habitat
196 assessment for the species of interest (Thorson et al., 2016; Grüss & Thorson, 2019; Han et
197 al., 2021; Grüss, Moore, et al., 2023): (1) density maps can be generated; (2) annual centres of
198 gravity (COGs) can be computed, to shed light on distribution shift patterns; and (3) changes
199 in effective area occupied and population boundaries over time can be evaluated, to determine
200 patterns of range expansion/contraction (Appendix S1). Eastward and northward COGs
201 represent, respectively, the weighted mean longitude and weighted mean latitude of the
202 species of interest in a given year, where each location of the modelled domain is weighted by
203 the species' biomass at that location in that year (Thorson et al., 2016). As such, COGs
204 contribute to highlight locations where species are faring well versus locations where this is
205 not the case; e.g., a substantial distribution shift to the east suggests the species is undergoing
206 depletion in some westernmost locations. Habitat assessments are not used as inputs in JARA
207 yet constitute valuable complementary information for Red List assessments to better
208 understand what may be driving species' extinction risk.

209

210 JARA

211 JARA is a generalised Bayesian state-space modelling tool that analyses one or several
212 indices simultaneously, to determine in which Red List category species are likely to fall
213 (Winker et al., 2020). In JARA, posterior distributions are estimated using Markov Chain
214 Monte Carlo simulation. Uninformative priors are employed for all estimable parameters so

215 that all the information on which inferences are based come from the indices considered and
 216 their associated uncertainty. For simplicity, we consider only the cases where one single
 217 VAST index is used in JARA.

218 In JARA, the trend of the indices is assumed to follow a Markovian process such that
 219 the index in year t , $I(t)$, is conditioned upon the index in year $t - 1$, $I(t - 1)$. A
 220 conventional exponential growth is assumed for the trend of the underlying population, such
 221 that the process equation on the log scale is:

$$\mu(t) = \mu(t - 1) + r(t - 1) \quad \text{eqn 1}$$

222 where $\mu(t) = \log(I(t))$; and $r(t) = \log(\lambda(t))$ is the annual rate of change, with $\lambda(t)$ being
 223 growth rate in year t , and is considered to follow a random walk:

$$r(t) = \bar{r} + \eta(t) - 0.5\sigma_\eta^2 \quad \text{eqn 2}$$

224 where \bar{r} is the estimable mean rate of change; and $\eta(t)$ is the process error following a zero-
 225 centered normal distribution with standard deviation σ_η^2 .

226 The observation equation corresponding to equation 1 is:

$$\log(y(t)) = \mu(t) + \varepsilon(t) \quad \text{eqn 3}$$

227 where $y(t)$ is the relative abundance observation in year t ; and $\varepsilon(t)$ is the log-normal
 228 observation error in year t . The observation variance is given by the sum of the inputted
 229 squared standard error estimates for the abundance index (here from VAST) and additional
 230 variance estimated by JARA. The Bayesian implementation of the state-space model and the
 231 diagnostics employed to evaluate it are described in Appendix S2.

232 The posterior of the population trajectory predicted by JARA, $\hat{I}(t) = \exp(\mu(t))$, is
 233 used to calculate a posterior probability for the percent change in the fish population (%C). If
 234 $\hat{I}(t)$ spans more than three generation lengths (GLs), %C is estimated as the difference
 235 between the three-year median around the final year of $\hat{I}(t)$, denoted T , and the three-year
 236 median around the year corresponding to $T - (3 \times GL)$ (Sherley et al., 2020). To diminish the

237 impact of short-term fluctuations, JARA always projects the year $T + 1$ to produce a three-
238 year median around T . When $\hat{I}(t)$ represents a time span smaller than three GLs, forward
239 projections are conducted in JARA; specifically, additional years without observations are
240 provided to JARA until $\hat{I}(t)$ spans a period greater than $(3 \times GL) + 2$. Projections are based
241 on the posterior of the median of $r(t)$ over all T years (Sherley et al., 2020).

242 JARA's main outcome is a graphic displaying the posterior distribution for %C over
243 three GLs against the thresholds for Red List categories under IUCN Criterion A2 (Appendix
244 S2). Another useful JARA outcome is retrospective analyses, where the terminal years of the
245 index $I(t)$ are sequentially removed and forward projections are subsequently carried out to
246 attain three GLs. These retrospective analyses allow for the identification of years in which
247 %C traversed new Red List categories (Winker et al., 2020).

248

249 COUPLING JARA WITH VAST

250 We demonstrate the benefits of coupling the state-of-the-art VAST and JARA
251 modelling tools through an application for five North Sea species. In particular, we show how
252 VAST, in addition to delivering an index (and its associated standard errors) to JARA, also
253 provides a habitat assessment that helps better interpret JARA outcomes. The five study
254 species represent contrasting fish populations: starry ray (*Amblyraja radiata*) and lesser-
255 spotted dogfish (*Scyliorhinus canicular*), elasmobranchs without a quantitative assessment
256 and which latest global Red List assessments found to be VU and LC, respectively; spurdog
257 (*Squalus acanthias*), an assessed elasmobranch species which latest global Red List
258 assessments found to be LC; and cod (*Gadus morhua*) and European plaice (*Pleuronectes*
259 *platessa*), assessed bony fishes which latest global Red List assessments found to be VU and
260 LC, respectively. (Table 1). The VAST models were fitted to the data that were collected by
261 the North Sea International Bottom Trawl Survey (NS-IBTS), which were retrieved from the

262 International Centre for the Exploration of the Sea (ICES) on their DATRAS platform
263 (DATRAS, 2023) to be made available in the FISHGLOB database (Maureaud et al., 2024)
264 (Appendix S3). None of the VAST models included density or catchability covariates. The
265 GLs used in JARA were those employed in the most recent Red List assessments for the study
266 species or were obtained from R package *FishLife* (Thorson, 2020) when not available in Red
267 List assessments (Appendix S4).

268 Our North Sea application using FISHGLOB showcases this large international
269 collaborative effort. FISHGLOB integrates scientific bottom trawl survey data collected
270 worldwide that are pre-processed and homogenised (Maureaud et al., 2024). Here, we focus
271 on the NS-IBTS survey data collected in Quarter 1 (January-March; NS-IBTS Q1) between
272 1983–2020 (DATRAS, 2023) that are available in the FISHGLOB database (Grüss, 2023),
273 while acknowledging some limitations of the NS-IBTS Q1 survey for some of the study
274 species (Appendix S4).

275 The authors of the present study did not conduct the research surveys themselves and,
276 therefore, ethical approval did not apply to the present study. All of the R codes developed for
277 the application are publicly available (Grüss, 2024).

278

279 **Results**

280 **STARRY RAY**

281 VAST predicted that starry ray relative biomass significantly decreased between
282 1983–2020 in the North Sea (Fig. 1). More specifically, VAST predicted that the starry ray
283 population increased until 1993 and sharply declined afterwards (Figs 1 and 2). VAST
284 predicted a dramatic habitat shrinkage for starry ray in the North Sea over the period 1983–
285 2020: the COG of starry ray was predicted to significantly move eastwards and its effective
286 area occupied to significantly diminish (Fig 1). VAST predicted that, in 2020, starry ray

287 density hotspots became concentrated in the east of the North Sea, particularly in the
288 Skagerrak Strait (Fig. 2).

289 JARA provided a percent change in the fish population (%C) estimate over three GLs
290 for starry ray of -88.3%, with 97% of the posterior falling in CR (Fig. 3 and Table 1).
291 Retrospective analyses with JARA suggested that starry ray switched from the CR status to
292 the EN status in the last two years of the period 1983–2020 (Appendix S4).

293

294 COD

295 VAST predicted a significant decrease in cod relative biomass between 1983–2020
296 (Appendix S4). More precisely, the cod population was predicted to considerably dwindle
297 until 2006, increase until 2016, and substantially decline again afterwards. VAST also
298 estimated that the COG of cod significantly moved northwards (as well as westwards)
299 between 1983–2020 and that the effective area occupied by the species significantly
300 diminished. Consequently, VAST predicted that, while cod high-density areas were found
301 throughout the North Sea in 1983, they tended to concentrate in the north of the region in
302 2020, particularly in the area between Shetland Islands and Scandinavia.

303 JARA provided a %C over three GLs for cod of -69.3%, with 100% of the posterior
304 falling in EN. The drop in cod relative biomass worsened in the most recent GL of 1983–2020
305 (Appendix S4). Retrospective analyses with JARA suggested that increases in the cod
306 population between 2006 and 2016 resulted in cod becoming LC in 2016, but that the large
307 decline in cod relative biomass afterwards led the threshold for the EN status to be exceeded
308 again in 2019–2020 (Fig. 4).

309

310 SPURDOG

311 VAST predicted an overall decline in spurdog relative biomass between 1983–2020
312 (Appendix S4). More precisely, the spurdog population was predicted to increase until 1990,
313 dwindle until 2010, and slightly increase afterwards. Its COG significantly moved northwards
314 between 1983–2020. The extent of spurdog high-density areas varied over time in response to
315 changes in population size. While spurdog density hotspots were located primarily around
316 Orkney Island in 1983, they were also found on the Fladen Ground and in the north of the
317 Skagerrak Strait in 2020.

318 JARA provided a %C estimate over three GLs for spurdog of -52.6%, with 53% of the
319 posterior falling in EN. Retrospective analyses with JARA suggested that increases in the
320 spurdog population after 2010 have resulted in spurdog switching from the CR status to the
321 EN status in 2013 (Appendix S4).

322

323 LESSER-SPOTTED DOGFISH

324 VAST predicted a very significant improvement in lesser-spotted dogfish relative
325 biomass between 1983–2020 (Appendix S4). The increase in relative biomass started from
326 1999 and accelerated after 2010. VAST also predicted that the effective area occupied by
327 lesser-spotted dogfish significantly diminished in 1983–2020 and that its COG significantly
328 moved southwards and eastwards. Thus, VAST predicted that the highest lesser-spotted
329 dogfish densities in 2020 were located in the eastern English Channel and southern North Sea.
330 JARA estimated that the lesser-spotted dogfish population was LC with a 100% probability
331 (Appendix S4).

332

333 EUROPEAN PLAICE

334 VAST predicted a significant improvement in European plaice relative biomass
335 between 1983–2020 (Appendix S4). More precisely, VAST predicted an increase between

336 2005 and 2015 followed by a decrease. VAST predicted that plaice COG significantly moved
337 westwards between 1983–2020 and that its density hotspots depended on the population
338 trajectory. JARA estimated a %C over three GLs for European plaice of +55.5%, with 100%
339 of the posterior falling in LC.

340

341 **Discussion**

342 Here, we showed the benefits of coupling the VAST and JARA modelling tools for
343 better informed Red List assessments of marine fishes. One primary advantage of the VAST-
344 JARA modelling framework is its adequate characterisation and communication of
345 uncertainty around extinction risks with the Bayesian JARA model, which is paramount for
346 making and prioritising conservation decisions. Moreover, VAST not only delivers indices to
347 JARA whose uncertainty is propagated to JARA outcomes, but also provides a habitat
348 assessment for each species which complements JARA outputs. We illustrated those two
349 advantages with an application to five North Sea species.

350 The North Sea application coupled with previous assessments and studies (Appendix
351 S4) suggest that, among the three study elasmobranchs, starry ray is in most need for urgent
352 research and management action where deemed appropriate (noting that it has been listed as
353 either a species not to be retained or a prohibited species on European Union fishing
354 regulations since 2014), followed by spurdog, whilst lesser-spotted dogfish is increasing in
355 biomass. We hasten to caveat that the NS-IBTS Q1 survey only partially covers the
356 distribution area of the stock of spurdog in the North Sea, which is considered to occupy the
357 whole of the Northeast Atlantic (ICES, 2022), and that some caution may therefore be
358 required when interpreting our results for spurdog. As the NS-IBTS Q1 survey does not fully
359 cover the spurdog stock and other stocks (e.g., the cod stocks as of 2023) that are considered
360 by ICES, we encourage the integration of data from different sources (collected by different

361 surveys and/or observer programs) in VAST in future applications of our VAST-JARA
362 modelling framework for North Sea species. The major issue with a survey that does not fully
363 cover stock units is that it does not allow for an accurate habitat assessment for those stock
364 units (Grüss, Charsley, et al., 2023). Integrating different data sources in VAST will allow for
365 improved habitat assessments, as well as for the generation of indices for JARA likely to have
366 reduced uncertainty and interannual variability and to cover a longer time period (Grüss,
367 Charsley, et al., 2023; Grüss, Thorson, et al., 2023). Data integration could be done with
368 seasonal VAST models allowing for the sharing of information not only across locations,
369 years and data sources, but also across seasons, to seek to further improve the quality of the
370 indices estimated with VAST (Thorson et al., 2020).

371 Moreover, both the VAST-JARA modelling framework and previous research
372 (Appendix S4) indicate that, while European plaice is not of conservation concern, cod has
373 likely met the IUCN criteria for being listed as Endangered (EN) recently. However, we
374 hasten to note that our data were for 1983–2020 and that a new stock assessment is upcoming
375 for cod at the time of the present study (in 2023), which will consider a new definition of the
376 Northern Shelf cod stocks and may provide different insights into the status of those stocks
377 (ICES, 2023).

378 The population trends estimated by JARA were supported by the patterns of spatial
379 density and distribution shifts predicted by VAST. The density maps and annual centres of
380 gravity produced with VAST help distinguish between the areas of the study region where the
381 species of interest is faring well from the areas where the species is undergoing depletion.
382 Such information is invaluable for guiding spatial management efforts, including the design of
383 marine protected areas (Grüss et al., 2019a; Paradinas et al., 2022). To further understand the
384 patterns of spatial density and distribution shifts predicted by VAST and better exploit this
385 information, we recommend research to determine the relative importance of fishing,

386 environmental variables, and multispecies interactions in explaining changes in density and
387 distribution shifts in starry ray and cod, noting that both are boreal species that may have
388 responded to increasing sea temperatures (Dulvy et al., 2008).

389 VAST also provided insights into the patterns of range expansion/contraction of the
390 study species, by predicting annual changes in effective area occupied and population
391 boundaries. The effective area occupied metric estimated by VAST is similar to the metrics
392 employed in the Red List assessments that relate species' range size and extinction risk (i.e.,
393 based on Criterion B), namely the Area of Occupancy and the Extent of Occurrence (Keith et
394 al., 2018). However, here, the population trend estimated with JARA did not always concur
395 with the changes in effective area occupied in VAST. Thus, while the effective area occupied
396 of the declining starry ray and cod was predicted to significantly diminish, the effective area
397 occupied of the thriving lesser-spotted dogfish was not predicted to increase but rather to
398 significantly decrease. Based on the above-mentioned results, we encourage research to
399 improve understanding of the relationship between range changes and population trends in
400 marine fishes and develop optimal IUCN range reduction thresholds for classifying
401 population declines based on species' range loss. This research will be important to uncover
402 the risks of misclassifying IUCN conservation status when Criterion B (geographic range) is
403 used instead of Criterion A (population change).

404 While the VAST-JARA modelling framework constitutes a robust tool that adequately
405 characterises uncertainty, we caution against unequivocally accepting its outcomes. We
406 recommend that specialists of Red List assessments and the fish population of interest should
407 be involved in any application of the modelling framework. VAST indices and JARA settings
408 should be proofed and verified by experts, including both fish ecologists and survey scientists.
409 Importantly, the VAST-JARA modelling framework is designed as a decision-support tool
410 and its output should not be taken as a final classification of extinction risk (Sherley et al.,

411 2020). Instead, predictions from the VAST-JARA modelling framework, including JARA
412 output and VAST habitat assessment, should be seen as supporting information to make
413 interpretations based on Red List guidelines before a decision on the final Red List
414 assessment outcome can be made (Lee et al., 2019; Sherley et al., 2020).

415 The predictions of the VAST-JARA modelling framework for North Sea species will
416 help decision-makers in their next Red List assessment for the North Sea. We foresee
417 applications of the VAST-JARA modelling framework to assist Red List assessments of
418 numerous other marine fishes worldwide. In addition to the utilisation of multiple data
419 sources in VAST, we also envision several avenues for future research including, among
420 others, the use of VAST indices for different regions in JARA to derive weighted global %C
421 estimates, the consideration of several species simultaneously in VAST and/or JARA, and
422 investigations of climate change impacts on species' extinction risks with the VAST-JARA
423 modelling framework (Appendix S5). The VAST-JARA modelling framework can be
424 implemented with only a few years of monitoring data, but requires a fair number of
425 encounter monitoring observations per year for VAST models for individual species. The
426 consideration of multiple species simultaneously in VAST would allow for the borrowing of
427 information across locations and years but also across species, thereby allowing for the
428 estimation of VAST indices and JARA extinction risks for data-limited Red List species for
429 which this is not possible with the current VAST-JARA modelling framework.

430

431 **Acknowledgments**

432 We thank very much Romain Frelat for assisting us in preparing survey data. We are
433 very grateful to José de Oliveira and Jim Ellis for their expert review and to Olaf Jensen, the
434 Editor (Tadeu Siqueira), the Associate Editor (Caren Barceló) and three anonymous reviewers
435 for their comments, which all considerably improved the quality of the manuscript. We also

436 thank very much Lydia Groves for all of her assistance during the reviewing and production
437 processes. Reference to trade names does not imply endorsement by the National Marine
438 Fisheries Service, NOAA. The scientific results and conclusions, as well as any views or
439 opinions expressed herein, are those of the author(s) and do not necessarily reflect those of
440 NOAA or the Department of Commerce.

441

442 **Conflict of interest statement**

443 None of the authors have a conflict of interest.

444 **Authors' Contributions**

445 Arnaud Grüss, Henning Winker and James T. Thorson conceived the study; Arnaud Grüss,
446 Henning Winker, James T. Thorson and Nathan Pacoureau developed the models; Arnaud
447 Grüss and Aurore Maureaud compiled the data; Arnaud Grüss, Nicola D. Walker and Nathan
448 Pacoureau compared the results for the application to results from previous assessments and
449 studies; Arnaud Grüss, Henning Winker, James T. Thorson, Nicola D. Walker, Aurore
450 Maureaud and Nathan Pacoureau analysed and discussed the results and contributed to the
451 manuscript.

452

453 **Data availability statement**

454 Data are available from the Figshare Digital Repository
455 <https://doi.org/10.6084/m9.figshare.22596799.v1> (Grüss, 2023). R codes are available from
456 GitHub at <https://github.com/agruss2/VAST-JARA-modelling-framework> and Zenodo at
457 <https://doi.org/10.5281/zenodo.10565146> (Grüss, 2024)

458

459 **References**

460 Adams, C. F., Brooks, E. N., Legault, C. M., Barrett, M. A., & Chevrier, D. F. (2021). Quota
461 allocation for stocks that span multiple management zones: Analysis with a vector
462 autoregressive spatiotemporal model. *Fisheries Management and Ecology*, 28(5),
463 417–427.

464 Ale, S. B., & Mishra, C. (2018). The snow leopard’s questionable comeback. *Science*,
465 359(6380), 1110–1110.

466 Boyd, C., DeMaster, D. P., Waples, R. S., Ward, E. J., & Taylor, B. L. (2017). Consistent
467 Extinction Risk Assessment under the U.S. Endangered Species Act. *Conservation*
468 *Letters*, 10(3), 328–336.

469 Brodie, S. J., Thorson, J. T., Carroll, G., Hazen, E. L., Bograd, S., Haltuch, M. A., Holsman,
470 K. K., Kotwicky, S., Samhouri, J. F., & Willis-Norton, E. (2020). Trade-offs in
471 covariate selection for species distribution models: A methodological comparison.
472 *Ecography*, 43(1), 11–24.

473 Butchart, S. H., Walpole, M., Collen, B., Van Strien, A., Scharlemann, J. P., Almond, R. E.,
474 Baillie, J. E., Bomhard, B., Brown, C., & Bruno, J. (2010). Global biodiversity:
475 Indicators of recent declines. *Science*, 328(5982), 1164–1168.

476 COSEWIC. (2019). *Committee on the Status of Endangered Wildlife in Canada*.
477 [https://cosewic.ca/images/cosewic/pdf/Instructions-for-status-report-writers-](https://cosewic.ca/images/cosewic/pdf/Instructions-for-status-report-writers-Nov2019_EN.pdf)
478 [Nov2019_EN.pdf](https://cosewic.ca/images/cosewic/pdf/Instructions-for-status-report-writers-Nov2019_EN.pdf).

479 da Silva, C., Winker, H., Parker, D., & Kerwath, S. (2019). Assessment of smoothhound
480 shark *Mustelus mustelus* in South Africa. *Report No.: DEFF/FISHERIES/LSWG/AUG*
481 *2019*. Cape Town, South Africa: Department of Agriculture, Forestry and Fisheries.

482 DATRAS. (2023). *ICES Database on Trawl Surveys (DATRAS)*. <https://datras.ices.dk>.

483 Davies, T. D., & Baum, J. K. (2012). Extinction risk and overfishing: Reconciling
484 conservation and fisheries perspectives on the status of marine fishes. *Scientific*
485 *Reports*, 2(1), 561.

486 Dennis, D., Plagányi, É., Van Putten, I., Hutton, T., & Pascoe, S. (2015). Cost benefit of
487 fishery-independent surveys: Are they worth the money? *Marine Policy*, 58, 108–115.

488 d'Eon-Eggertson, F., Dulvy, N. K., & Peterman, R. M. (2015). Reliable identification of
489 declining populations in an uncertain world. *Conservation Letters*, 8(2), 86–96.

490 Dulvy, N. K., Pacoureaux, N., Rigby, C. L., Pollom, R. A., Jabado, R. W., Ebert, D. A.,
491 Finucci, B., Pollock, C. M., Cheok, J., & Derrick, D. H. (2021). Overfishing drives
492 over one-third of all sharks and rays toward a global extinction crisis. *Current Biology*,
493 31(21), 4773–4787.

494 Dulvy, N. K., Rogers, S. I., Jennings, S., Stelzenmüller, V., Dye, S. R., & Skjoldal, H. R.
495 (2008). Climate change and deepening of the North Sea fish assemblage: A biotic
496 indicator of warming seas. *Journal of Applied Ecology*, 45(4), 1029–1039.

497 Grüss, A. (2023). Data from: Coupling state-of-the-art modelling tools for better informed
498 Red-List assessments of marine fishes. Figshare.
499 <https://doi.org/10.6084/m9.figshare.22596799.v1>.

500 Grüss, A. (2024). VAST-JARA modelling framework v1.0. Zenodo.
501 <https://doi.org/10.5281/zenodo.10565146>.

502 Grüss, A., Biggs, C. R., Heyman, W. D., & Erisman, B. (2019a). Protecting juveniles,
503 spawners or both: A practical statistical modelling approach for the design of marine
504 protected areas. *Journal of Applied Ecology*, 56(10), 2328–2339.

505 Grüss, A., Charsley, A. R., Thorson, J. T., Anderson, O. F., O'Driscoll, R. L., Wood, B.,
506 Breivik, O. N., & O'Leary, C. A. (2023). Integrating survey and observer data

507 improves the predictions of New Zealand spatio-temporal models. *ICES Journal of*
508 *Marine Science*, 80(7), 1991–2007.

509 Grüss, A., Moore, B. R., Pinkerton, M. H., & Devine, J. A. (2023). Understanding the spatio-
510 temporal abundance patterns of the major bycatch species groups in the Ross Sea
511 region Antarctic toothfish (*Dissostichus mawsoni*) fishery. *Fisheries Research*, 262,
512 106647.

513 Grüss, A., & Thorson, J. T. (2019). Developing spatio-temporal models using multiple data
514 types for evaluating population trends and habitat usage. *ICES Journal of Marine*
515 *Science*, 76(6), 1748–1761.

516 Grüss, A., Thorson, J. T., Anderson, O. F., O’Driscoll, R., Heller-Shiple, M., & Goodman,
517 S. (2023). Spatially varying catchability for integrating research survey data with other
518 data sources: Case studies involving observer samples, industry-cooperative surveys,
519 and predators-as-samplers. *Canadian Journal of Fisheries and Aquatic Sciences*,
520 80(10), 1595–1615.

521 Grüss, A., Walter III, J. F., Babcock, E. A., Forrestal, F. C., Thorson, J. T., Laretta, M. V., &
522 Schirripa, M. J. (2019b). Evaluation of the impacts of different treatments of spatio-
523 temporal variation in catch-per-unit-effort standardization models. *Fisheries Research*,
524 213, 75–93.

525 Han, Q., Grüss, A., Shan, X., Jin, X., & Thorson, J. T. (2021). Understanding patterns of
526 distribution shifts and range expansion/contraction for small yellow croaker
527 (*Larimichthys polyactis*) in the Yellow Sea. *Fisheries Oceanography*, 30(1), 69–84.

528 Hodgdon, C. T., Tanaka, K. R., Runnebaum, J., Cao, J., & Chen, Y. (2020). A framework to
529 incorporate environmental effects into stock assessments informed by fishery-
530 independent surveys: A case study with American lobster (*Homarus americanus*).
531 *Canadian Journal of Fisheries and Aquatic Sciences*, 77(10), 1700–1710.

532 Hoffmann, M., Brooks, T. M., Da Fonseca, G. A. B., Gascon, C., Hawkins, A. F. A., James,
533 R. E., Langhammer, P., Mittermeier, R. A., Pilgrim, J. D., & Rodrigues, A. S. L.
534 (2008). Conservation planning and the IUCN Red List. *Endangered Species Research*,
535 6(2), 113–125.

536 Hoyle, S. D., Campbell, R. A., Ducharme-Barth, N. D., Grüss, A., Moore, B. R., Thorson, J.
537 T., Tremblay-Boyer, L., Winker, H., Zhou, S., & Maunder, M. N. (2024). Catch per
538 unit effort modelling for stock assessment: A summary of good practices. *Fisheries*
539 *Research*, 269, 106860.

540 ICES. (2022). Spurdog (*Squalus acanthias*) in subareas 1–10, 12, and 14 (the Northeast
541 Atlantic and adjacent waters). In *Report of the ICES Advisory Committee, 2022. ICES*
542 *Advice 2022, dgs.27.nea*. <https://doi.org/10.17895/ices.advice.19753588>.

543 ICES. (2023). Benchmark workshop on Northern Shelf cod stocks (WKBCOD). *ICES*
544 *Scientific Reports*. 5:37. 425 pp. <https://doi.org/10.17895/ices.pub.22591423>.

545 IUCN. (2023). *The IUCN Red List of Threatened Species. Version 2022-2*.
546 <https://www.iucnredlist.org>.

547 Keith, D. A., Akçakaya, H. R., & Murray, N. J. (2018). Scaling range sizes to threats for
548 robust predictions of risks to biodiversity. *Conservation Biology*, 32(2), 322–332.

549 Lee, C. K., Keith, D. A., Nicholson, E., & Murray, N. J. (2019). Redlistr: Tools for the IUCN
550 Red Lists of ecosystems and threatened species in R. *Ecography*, 42(5), 1050–1055.

551 Lo, N. C., Jacobson, L. D., & Squire, J. L. (1992). Indices of relative abundance from fish
552 spotter data based on delta-lognormal models. *Canadian Journal of Fisheries and*
553 *Aquatic Sciences*, 49(12), 2515–2526.

554 Mace, G. M., Collar, N. J., Gaston, K. J., Hilton-Taylor, C., Akçakaya, H. R., Leader-
555 Williams, N., Milner-Gulland, E. J., & Stuart, S. N. (2008). Quantification of

556 extinction risk: IUCN's system for classifying threatened species. *Conservation*
557 *Biology*, 22(6), 1424–1442.

558 Maunder, M. N., & Punt, A. E. (2004). Standardizing catch and effort data: A review of
559 recent approaches. *Fisheries Research*, 70(2–3), Article 2–3.

560 Maureaud, A. A., Palacios-Abrantes, J., Kitchel, Z., Mannocci, L., Pinsky, M. L., Fredston,
561 A., Beukhof, E., Forrest, D. L., Frelat, R., & Palomares, M. L. (2024).
562 FISHGLOB_data: An integrated dataset of fish biodiversity sampled with scientific
563 bottom-trawl surveys. *Scientific Data*, 11(1), 24.

564 National Research Council. (1998). *Improving fish stock assessments*. Washington, DC:
565 National Academy Press.

566 O'Leary, C. A., Thorson, J. T., Ianelli, J. N., & Kotwicki, S. (2020). Adapting to climate-
567 driven distribution shifts using model-based indices and age composition from
568 multiple surveys in the walleye pollock (*Gadus chalcogrammus*) stock assessment.
569 *Fisheries Oceanography*, 29(6), 541–557.

570 Ovando, D., Hilborn, R., Monnahan, C., Rudd, M., Sharma, R., Thorson, J. T., Rousseau, Y.,
571 & Ye, Y. (2021). Improving estimates of the state of global fisheries depends on better
572 data. *Fish and Fisheries*, 22(6), 1377–1391.

573 Pacoureau, N., Carlson, J. K., Kindsvater, H. K., Rigby, C. L., Winker, H., Simpfendorfer, C.
574 A., Charvet, P., Pollom, R. A., Barreto, R., & Sherman, C. S. (2023). Conservation
575 successes and challenges for wide-ranging sharks and rays. *Proceedings of the*
576 *National Academy of Sciences*, 120(5), e2216891120.

577 Pacoureau, N., Rigby, C. L., Kyne, P. M., Sherley, R. B., Winker, H., Carlson, J. K.,
578 Fordham, S. V., Barreto, R., Fernando, D., & Francis, M. P. (2021). Half a century of
579 global decline in oceanic sharks and rays. *Nature*, 589(7843), 567–571.

580 Paradinas, I., Giménez, J., Conesa, D., López-Quílez, A., & Pennino, M. G. (2022). Evidence
581 for spatiotemporal shift in demersal fishery management priority areas in the western
582 Mediterranean. *Canadian Journal of Fisheries and Aquatic Sciences*, 79(10), 1641–
583 1654.

584 Post, J. R., Ward, H. G. M., Wilson, K. L., Sterling, G. L., Cantin, A., & Taylor, E. B. (2022).
585 Assessing conservation status with extensive but low-resolution data: Application of
586 frequentist and Bayesian models to endangered Athabasca River rainbow trout.
587 *Conservation Biology*, 36(3), e13783.

588 RAM Legacy Stock Assessment Database. (2021). *RAM Legacy Stock Assessment Database*
589 *v4.495 (v4.495)*. <https://doi.org/10.5281/zenodo.4824192>.

590 Regan, T. J., Taylor, B. L., Thompson, G. G., Cochrane, J. F., Ralls, K., Runge, M. C., &
591 Merrick, R. (2013). Testing decision rules for categorizing species' extinction risk to
592 help develop quantitative listing criteria for the US Endangered Species Act.
593 *Conservation Biology*, 27(4), 821–831.

594 Rueda-Cediel, P., Anderson, K. E., Regan, T. J., & Regan, H. M. (2018). Effects of
595 uncertainty and variability on population declines and IUCN Red List classifications.
596 *Conservation Biology*, 32(4), 916–925.

597 Shelton, A. O., Thorson, J. T., Ward, E. J., & Feist, B. E. (2014). Spatial semiparametric
598 models improve estimates of species abundance and distribution. *Canadian Journal of*
599 *Fisheries and Aquatic Sciences*, 71(11), 1655–1666.

600 Sherley, R. B., Winker, H., Rigby, C. L., Kyne, P. M., Pollom, R., Pacoureau, N., Herman,
601 K., Carlson, J. K., Yin, J. S., & Kindsvater, H. K. (2020). Estimating IUCN Red List
602 population reduction: JARA—A decision-support tool applied to pelagic sharks.
603 *Conservation Letters*, 13(2), e12688.

604 Thorson, J. T. (2019). Guidance for decisions using the Vector Autoregressive Spatio-
605 Temporal (VAST) package in stock, ecosystem, habitat and climate assessments.
606 *Fisheries Research*, 210, 143–161.

607 Thorson, J. T. (2020). Predicting recruitment density dependence and intrinsic growth rate for
608 all fishes worldwide using a data-integrated life-history model. *Fish and Fisheries*,
609 21(2), 237–251.

610 Thorson, J. T., Adams, C. F., Brooks, E. N., Eisner, L. B., Kimmel, D. G., Legault, C. M.,
611 Rogers, L. A., & Yasumiishi, E. M. (2020). Seasonal and interannual variation in
612 spatio-temporal models for index standardization and phenology studies. *ICES*
613 *Journal of Marine Science*, 77(5), 1879–1892.

614 Thorson, J. T., Maunder, M. N., & Punt, E. (2020). The development of spatio-temporal
615 models of fishery catch-per-unit-effort data to derive indices of relative abundance.
616 *Fisheries Research*, 230, 105611.

617 Thorson, J. T., Pinsky, M. L., & Ward, E. J. (2016). Model-based inference for estimating
618 shifts in species distribution, area occupied and centre of gravity. *Methods in Ecology*
619 *and Evolution*, 7(8), 990–1002.

620 Thorson, J. T., Shelton, A. O., Ward, E. J., & Skaug, H. J. (2015). Geostatistical delta-
621 generalized linear mixed models improve precision for estimated abundance indices
622 for West Coast groundfishes. *ICES Journal of Marine Science*, 72(5), 1297–1310.

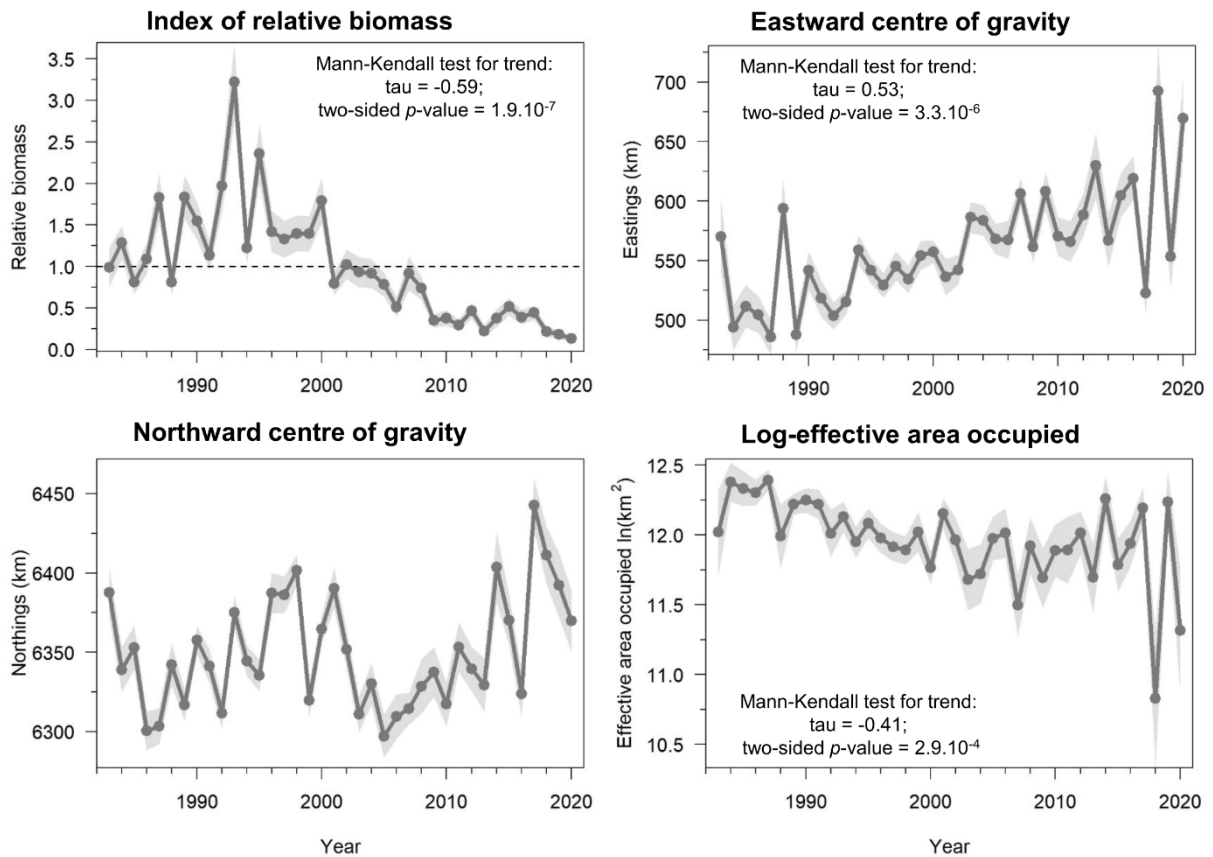
623 Wilson, K. L., Sawyer, A. C., Potapova, A., Bailey, C. J., LoScerbo, D., Sweeney-Bergen, E.
624 K., Hodgson, E. E., Pitman, K. J., Seitz, K. M., Law, L. K., Warkentin, L., Wilson, S.
625 M., Atlas, W. I., Braun, D. C., Sloat, M. R., Tinker, M. T., & Moore, J. W. (2023).
626 The role of spatial structure in at-risk metapopulation recoveries. *Ecological*
627 *Applications*, 33(6), e2898.

628 Winker, H., Pacoureau, N., & Sherley, R. B. (2020). JARA: 'Just Another Red-List
629 Assessment.' *BioRxiv*, 672899.

630

631 **Figures**

632 **Fig. 1.** Results of the VAST model for starry ray (*Amblyraja radiata*). Shaded areas represent
633 95% confidence intervals.



634 **Fig. 2.** Spatial patterns of log-density (in $\log(\text{kg}\cdot\text{km}^{-2})$) in select years of the period 1983-2020
635 predicted by the VAST model for starry ray. Spatial patterns of log-density in each year are
636 shown only for those areas where log-density is greater than 1% of the maximum expected
637 log-density over the entire period 1983-2020. For each year, the areas where log-density is
638 less than 1% of the maximum expected log-density over the entire period 1983-2020 are
639 highlighted in light grey.

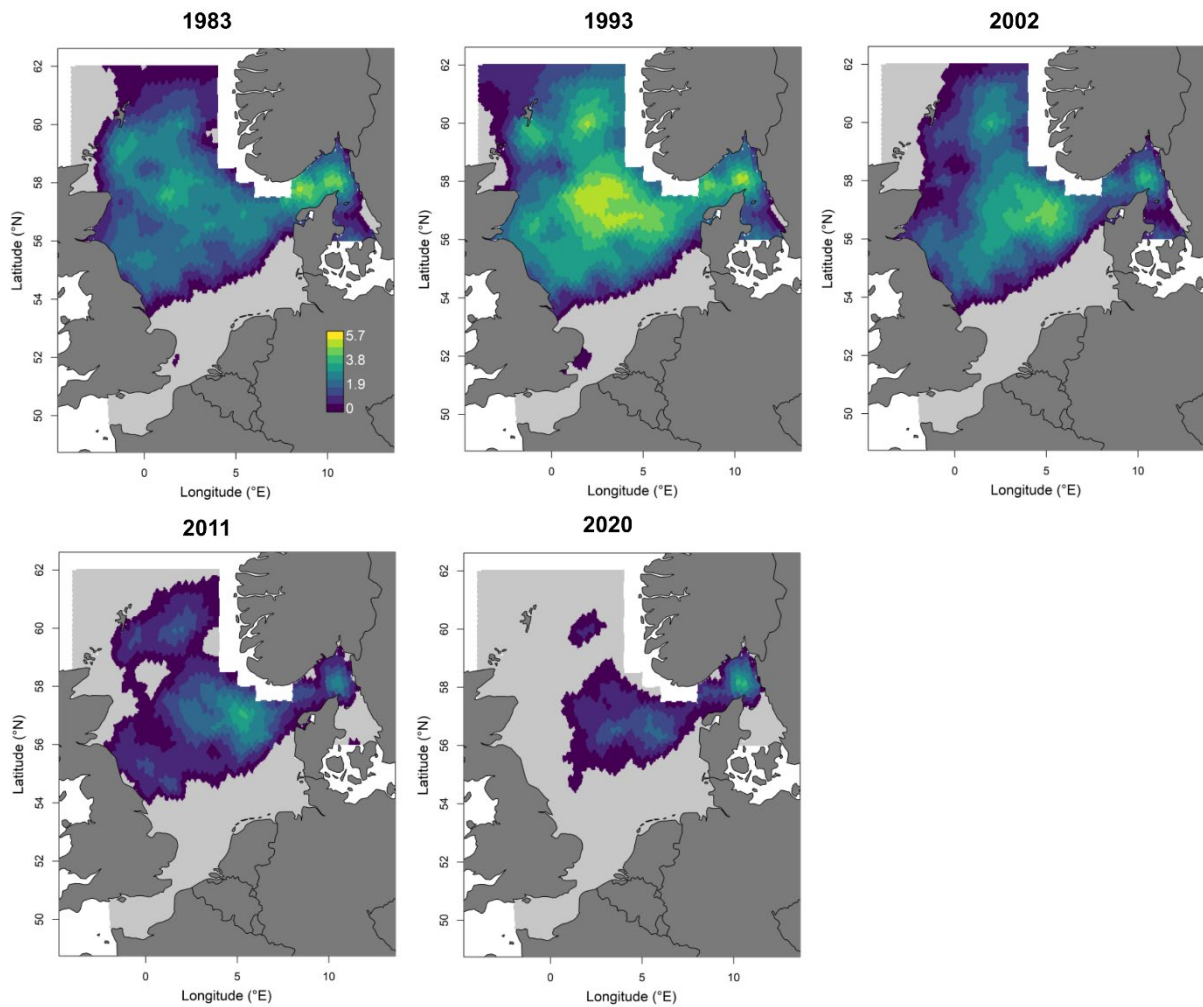
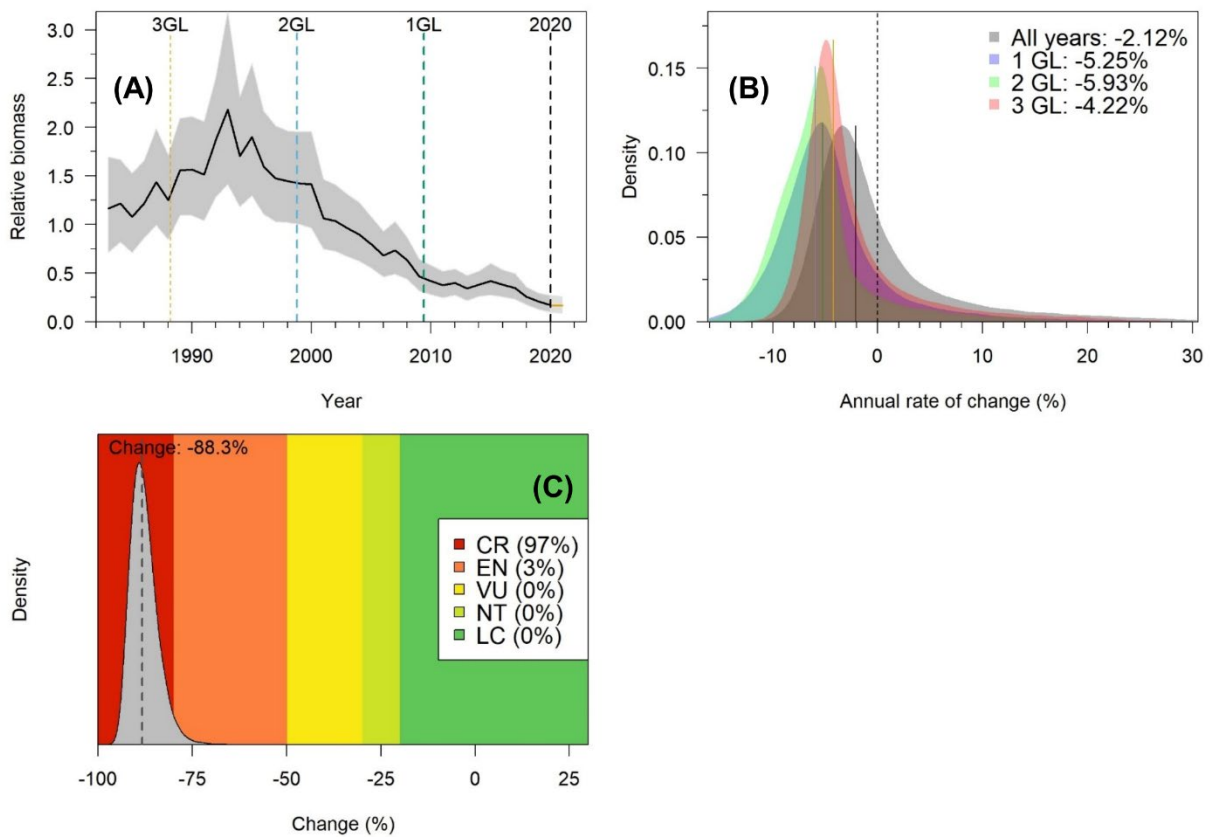
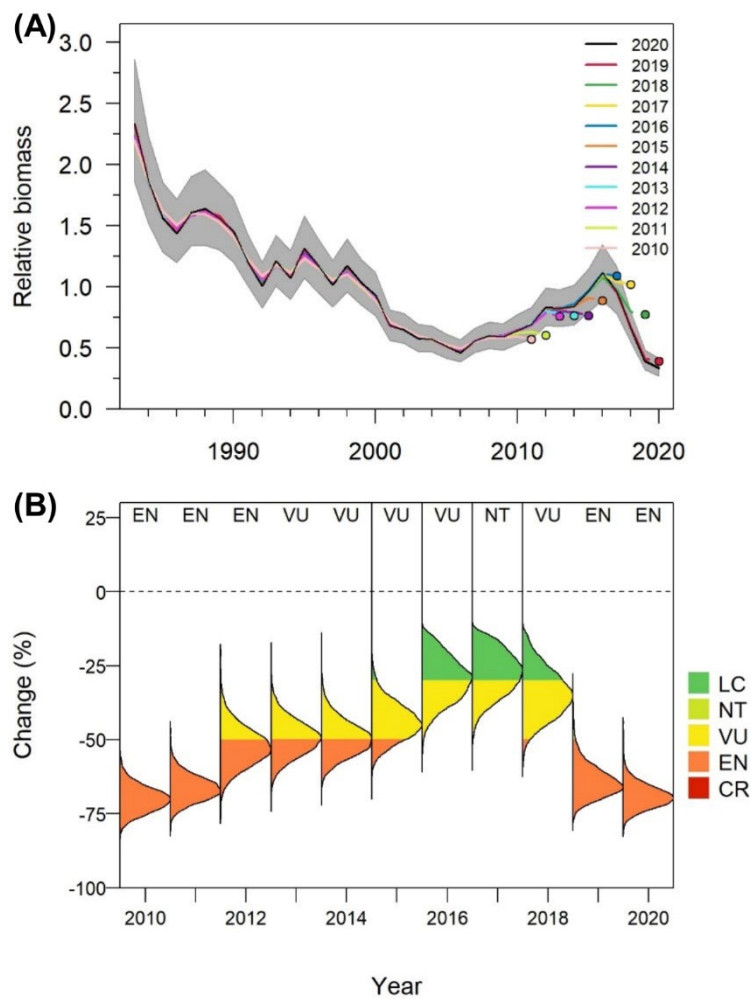


Fig. 3. Results of the JARA model for starry ray: (A) overall JARA fit (black line) to the VAST time-series and projected (dashed orange line) population trajectory over three generation lengths (GLs), and their 95% credible intervals (shaded areas); (B) the median and posterior probabilities for the percent annual change in the fish population (%C) calculated from all VAST years (in black), from the last 1 GL (in blue), from the last 2 GLs (in green) and from the last 3 GLs (in red), displayed relative to a stable population (with a %C of 0%; dotted line); (C) probabilities for %C over three GLs to fall within the International Union for the Conservation of Nature Red List categories under Red List Criterion A2 (also provided is the median %C over three GLs).



640 **Fig. 4.** Results of the retrospective analysis with JARA for cod (*Gadus morhua*): (A)
 641 retrospective pattern of relative biomass obtained through sequential removal of terminal
 642 years and subsequent forward projections to attain three generation lengths (GLs); and (B)
 643 corresponding retrospective status posteriors of change over three GLs – coloured according
 644 to the International Union for the Conservation of Nature Red List categories under Red List
 645 Criterion A2.



646 **Tables**

647 **Table 1.** Study species: regional (North Sea) name, International Union for the Conservation
 648 of Nature (IUCN) name, stock assessment information, and Red List category according to
 649 the most recent global Red List assessment and this study.

Species	IUCN species name	Has a quantitative stock assessment?	Red List category according to the most recent global Red List assessment	Red List category in this study
Starry ray (<i>Amblyraja radiata</i>)	Thorny Skate	No	VU	CR (97%), EN (3%)
Cod (<i>Gadus morhua</i>)	Atlantic Cod	Yes	VU	EN (100%)
Spurdog (<i>Squalus acanthias</i>)	Spiny Dogfish	Yes	VU	CR (2%), EN (53%), VU (26%), NT (7%), LC (12%)
Lesser-spotted dogfish (<i>Scyliorhinus canicula</i>)	Smallspotted Catshark	No	LC	LC (100%)
European plaice (<i>Pleuronectes platessa</i>)	European Plaice	Yes	LC	LC (100%)